(Sub)nanosecond transient plasma for atmospheric plasma processing experiments: application to ozone generation and NO removal

(Sub)nanosecond transient plasma for atmospheric plasma processing experiments: application to ozone generation and NO removal

T Huiskamp, W F L M Hoeben, F J C M Beckers, E J M van Heesch and A J M Pemen

Department of Electrical Engineering, Electrical Energy Systems group, Eindhoven University of Technology, PO Box 513, 5600 MB Eindhoven, The Netherlands

E-mail: t.huiskamp@tue.nl

Abstract.

In this paper we use a (sub)nanosecond high-voltage pulse source (2–9 ns pulses with 0.4 ns rise time) to generate streamer plasma in a wire-cylinder reactor and apply it to two atmospheric plasma processing applications: ozone generation and NO removal. We will investigate what pulse parameters result in the highest plasma processing yields.

The results show that for ozone generation, secondary-streamer effects appear to have a slight influence on the ozone yield: if the pulse duration increases and/or the voltage increases in such a way that streamers can start to cross the gap in the reactor, the ozone yields decrease. Furthermore, for NO removal, we see a similar effect of pulse duration and applied voltage as for the ozone generation, but the effect of the pulse duration is slightly different: long pulses result in the highest NO-removal yield. However, the NO-removal process is fundamentally different: besides removing NO, the plasma also produces NO and this production is more pronounced in the primary-streamer phase, which is why the pulse polarity has almost no influence on the NO-removal yield (only on the by-product formation). Moreover, the rise time of the pulses has a much more significant effect on ozone generation and NO removal than the pulse duration: a long rise time results in a lower enhanced electric field at the streamer heads, which consequently reduces the production of radicals required for ozone generation and NO removal, and decreases the streamer volume. Consequently, the resulting ozone yields and NO-removal yields are lower. Finally, the main conclusion is that the plasma generated with our nanosecond pulses is very efficient for ozone generation and NO removal, achieving yields as high as 175 $g \cdot kWh^{-1}$ for ozone generation and 2.5 $mol \cdot kWh^{-1}$ (or 14.9 eV per NO molecule) for NO removal.

1. Introduction

Transient plasmas generated by high-voltage pulses have been widely studied and used for industrial and environmental applications for more than 100 years [1, 2]. Due to the fast electrons that are generated by these non-thermal plasmas, they are very efficient in producing highly reactive radical species [1, 3]. These radicals can consequently react with, for instance, particles in gas streams (for example, pollutants, odour and dust), contamination in water, biological tissue, and material surfaces [4, 1]. In our research, we focus on using transient plasma for air purification applications [5].

Air purification is a technology that has been extensively studied for many kinds of non-thermal plasma — such as dielectric barrier discharges (DBDs), corona streamer plasmas, gliding arc discharges, etc. — and many kinds of air-purification applications [1]. In fact, the studies would be much too numerous to list in this introduction. What this shows is that the topic is actively researched, but also that no final solution or an optimal technology has been found for all applications. One of the main underlying reasons is that not each air-purification application benefits from the same type of plasma conditions. For example, naphthalene removal (a biomass gasification tar) benefits from a high process temperature [6], whereas ozone production decreases at high temperatures [7, 8].

In our work, we use short high voltage pulses to generate transient plasma, because recent research has shown that transient plasmas generated by very short nanosecond high-voltage pulses are very efficient for a variety of applications [9, 10, 11, 12, 13, 14, 15, 16]. Some researches have shown that the pulse duration of the applied high-voltage pulse has a significant influence on the radical yield of the transient plasmas generated with these pulses (shorter pulses result in higher yields) [9, 15, 10, 11]. However, the pulses that have been used for plasma generation so far are either still relatively long (>10 ns), have a long rise time (several nanoseconds), and/or are not square-shaped. Furthermore, a parametric study to investigate the effect of the pulse duration, rise time, and voltage (amplitude and polarity) is lacking (but strongly needed) for these short pulses.

In this paper, we will investigate air purification applications using short high voltage pulses (2–9 ns with 0.4 ns rise time) from a (sub)nanosecond high voltage pulse source that we recently developed [17, 18, 19, 20]. More specifically, we will investigate what pulse parameters result in the highest plasma processing yields.

1.1. Plasma processes

An obvious choice to make is: to which application do we apply our nanosecond pulse technology? Some of the classical air-purification processes are the production of ozone [21, 22, 23, 8, 24] and the removal/conversion of nitrogen oxides (NO_x) [25, 26, 21, 27, 28, 29, 16, 30], sulfur oxides (SO_x) [27, 31, 32, 33], volatile organic compounds (VOCs) [34, 35, 36, 37], tar [6, 38], odour [39, 40, 41], particulate matter (PM) [27, 41] and biological particles [41, 42, 43, 44, 45].

Of all the plasma processes, ozone generation and NO_x removal/conversion are most often used by researchers as a monitor for their plasma performance. For this reason we chose ozone production and NO removal as the main plasma processes to apply our nanosecond pulse technology to.

1.1.1. Ozone generation Strictly speaking, ozone generation is not purely an air-purification process, as its main use is cleaning polluted water [46]. However, the ozone in this cleaning process is mainly produced with non-thermal plasma. Especially DBD-plasmas are often used because of their ease of construction and design [2]. Nonetheless, ozone production remains one of the favourite processes to measure the performance of a plasma with, because it is an indirect measure for oxygen radical production [9]. It is for this reason that we chose ozone production as the first plasma process.

To generate ozone with a plasma in pure oxygen, an oxygen molecule first has to be dissociated by electron impact (at an energy cost ΔW).

$$O_2 + e \rightarrow O + O + e \qquad \Delta W = 5.2\,\text{eV} \tag{1}$$

The atomic oxygen then react with oxygen and a third collision partner (M) to form ozone:

$$O + O_2 + M \rightarrow O_3 + M. \tag{2}$$

When the feeding gas is not pure oxygen, but synthetic air, part of the available energetic electrons that are generated by the plasma will be used for excitation and dissociation of nitrogen.

$$N_2 + e \rightarrow N_2(A^3\Sigma_u^+) + e \qquad \Delta W = 6.2\,\text{eV} \tag{3}$$

$$N_2 + e \rightarrow N + N + e \qquad \Delta W = \sim 9.8\,\text{eV} \tag{4}$$

Some of the excited nitrogen species can again form atomic oxygen, but (part of) the atomic nitrogen will result in the formation of by-products that do not contribute to ozone formation or even lead to the destruction of ozone. A very extensive overview of ozone generation is given in [47, Section 2.5].

The yields of ozone generation in air that researchers report are generally in the range of 15–150 g·kWh^{-1} [21, 48, 7, 22, 24] for different types of plasmas and reactor configurations. Wang *et al.* report yields as high as 239 g·kWh^{-1}‡ with their nanosecond pulse source and show in an extensive map the comparisons between different discharge methods and the very good results of nanosecond pulsed discharges [49]. In [50] we already showed that the ozone yield with our nanosecond pulse source and our corona-plasma reactor can reach 170-190 g·kWh^{-1}, indicating that we obtain very high ozone yields as well.

‡ They calculate their ozone yields (and NO removal yields) at a temperature of 0° C and therefore overestimate the yields by almost 10 percent. However, the results are still excellent.

1.1.2. NO removal The release of NO_x into the environment due to the combustion of fossil fuels is still a major environmental problem and is strictly controlled by rules and regulations. Consequently, the possibility of non-thermal plasmas to reduce the amount of NO_x makes it one of the most studied air-purification applications in the field of plasma processing.

Just as with ozone production, the first step in the NO-removal process is the generation of radicals by the plasma. The experiments are all performed in synthetic air, so the plasma generates atomic oxygen and excited nitrogen species and atoms. The interaction of these species with NO and the associated by-products are complex and we only mention some of the important reaction pathways here [51, 7, 52].

When NO is present in the gas, the reactions that convert NO to other species in the presence of the plasma are:

$$NO + O + M \rightarrow NO_2 + M, \quad (5)$$

$$NO + N \rightarrow N_2 + O, \quad (6)$$

$$2NO + O_2 \rightarrow 2NO_2, \quad (7)$$

$$NO + O_3 \rightarrow NO_2 + O_2, \quad (8)$$

where the ozone in (8) is formed through (2). During this period the concentration of NO_2 increases as the concentration of NO decreases. At the same time, by-products N_2O and N_2O_5 are formed from NO_2 through

$$NO_2 + N \rightarrow N_2O, \quad (9)$$

$$NO_2 + O_3 \rightarrow NO_3 + O_2, \quad (10)$$

$$NO_2 + NO_3 + M \rightarrow N_2O_5 + M. \quad (11)$$

Consequently, once NO is removed, O_3, NO_2, N_2O and N_2O_5 will be the main by-products. The by-product NO_2 can be further removed from the gas by increasing the energy density of the plasma considerably. However, this increases the formation of the other by-products. Therefore, a corona plasma alone is not enough to remove all pollutants from an air stream.

In a real NO-removal application the air will not be dry synthetic air (as we use), but will contain significant amounts of H_2O. In the presence of H_2O, N_2O_5 and NO_2 will be converted to HNO_3 through

$$H_2O + N_2O_5 \rightarrow 2HNO_3, \quad (12)$$

$$NO_2 + OH + M \rightarrow HNO_3 + M. \quad (13)$$

The formed HNO_3 can then be removed by subsequent water-scrubbing technology or by an additional chemical reactor [52]. Further reduction of the by-products could be realised by in-plasma or post-plasma catalysis [53, 54, 55]. In this paper we will show NO concentrations, as well as concentrations of the by-products, but mainly focus on the NO-removal efficiency.

Unfortunately, besides converting NO to other compounds, the plasma also generates NO. Two important reactions that produce new NO with atomic oxygen and

atomic nitrogen are

$$N + O \quad \rightarrow NO, \tag{14}$$

$$NO_2 + O \rightarrow NO + O_2. \tag{15}$$

As we mentioned earlier, NO_x reduction is perhaps one of the most studied air-purification applications. Consequently, the reported removal efficiencies are diverse. Some examples that are worth mentioning are that of Matsumoto *et al.* [12] and Van Veldhuizen *et al.* [25]. Matsumoto *et al.* use the same type of 2-ns and 5-ns triaxial Blumlein source as used by Wang *et al.* (who reported the very high ozone yields) and reported NO-removal efficiencies of up to 1.2 mol·kWh^{-1} (equal to a cost of 31 eV per NO molecule) at 50 percent NO removal with an initial NO concentration of 200 ppm (again overestimating the yield). Van Veldhuizen *et al.* performed NO-removal experiments (300 ppm initial NO concentration) at elevated gas temperatures and achieved 50 percent NO removal at a cost of 20 eV per NO molecule (equal to 1.8 mol·kWh^{-1}). While these results are very good, most studies report much lower NO-removal efficiencies.

2. Experimental setup

In this section we describe the experimental setup that we used for the plasma-processing experiments. We used two different pulse sources: the (sub)nanosecond pulse source and a more conventional (nanosecond) pulse source. Furthermore we used two types of quantitative gas diagnostics: UV-absorption spectrometry for ozone measurements and FT-IR (Fourier Transform Infrared) absorption spectrometry for the NO_xexperiments.

2.1. Corona-plasma reactor

The corona-plasma reactor that we used in all the experiments of this paper is a 1-m coaxial wire-cylinder reactor (with a 0.5-mm diameter HV wire electrode), which we introduced in [50]. It is shown in Fig. 1. The reactor is connected to the nanosecond pulse source with a coaxial cable via a cable coupler.

2.2. Nanosecond pulse source

For the majority of the experiments in this paper we used the nanosecond pulse source that we recently developed at Eindhoven University of Technology. It is a single line pulse source, consisting of a pulse forming line that is charged by a microsecond pulse charger and is subsequently discharged by an oil spark gap. The generated pulse travels over a transmission line (a SA24272 coaxial cable) to the load, the corona reactor, where it produces a sufficiently high electric field to generate a streamer discharge. The coaxial cable adds a delay to the high-voltage pulses and is required for synchronisation of equipment such as an ICCD camera. The full design of this system is described in [17, 18, 19, 20] and is schematically presented in Fig. 2. The output pulses from the nanosecond pulse source (50-Ω output impedance) have an adjustable amplitude of

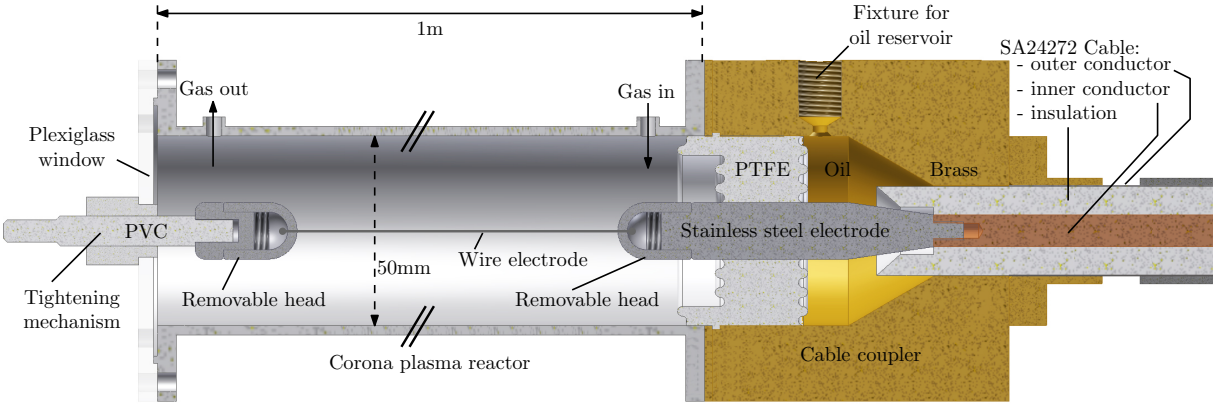

Figure 1: The corona-plasma reactor (not drawn to scale). On the right side of the sketch, the SA24272 coaxial cable from the nanosecond pulse source is connected to the a cable coupler. The cable coupler is oil-filled for high voltage insulation. The inner conductor of the cable is connected to a stainless-steel electrode with a removable head. The reactor is connected to the cable coupler and the wire electrode is strung between the removable heads of the electrode and the tightening mechanism.

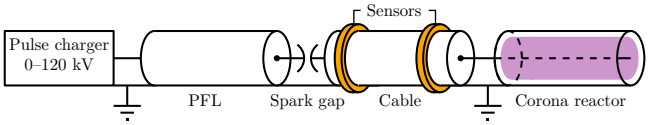

Figure 2: Schematic of the single line pulse source. The pulse charger charges the pulse forming line (PFL) which is then discharged by the spark gap into a matched cable. When the voltage pulse reaches the corona reactor it generates a streamer discharge. B-dot and D-dot sensors are integrated on the cable to measure voltage and current waveforms. Reproduced from [57].

3–50 kV (positive and negative), an adjustable pulse duration of 0.5–10 ns and a rise time of less than 200 ps. Once the pulses reach the plasma reactor, the pulses have a rise time of around 400 ps due to attenuation and dispersion in the SA24272 cable [18].

On the SA24272 coaxial cable that connects the plasma reactor to the pulse source, we mounted B-dot and D-dot sensors to measure the current and voltage of the high-voltage pulses respectively. The full design, calibration and implementation of these sensors is described in a previous paper [56]. Figure 3 shows some example waveforms of the output of the nanosecond pulse source measured with these sensors. We calculate the energy that is dissipated in the plasma from the voltage and current waveforms measured at the side of the plasma reactor. For each measurement point, we average over 250 pulses§.

§ This averaging is required because the amplitude of the output voltage of the nanosecond pulse source is not exactly the same for each pulse. This standard deviation on the amplitude (around 10% of the average amplitude) is caused by the oil spark gap in the pulse source (see [18]).

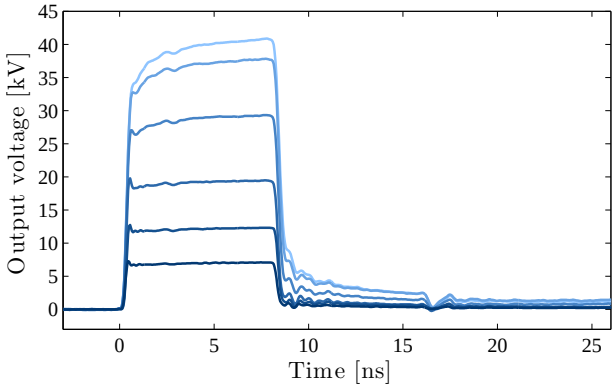

(a)

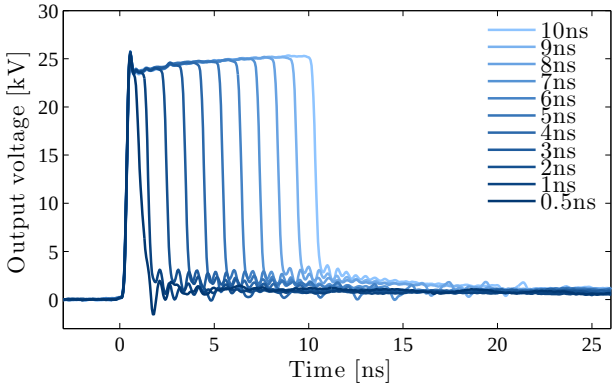

(b)

Figure 3: Example waveforms of the nanosecond pulse source. (a) A 8-ns pulse with different amplitudes. (b) A 25-kV pulse with different pulse durations.

2.3. Conventional pulse source

In [55] we presented a more conventional pulse source. We used it for some of the experiments in this paper to be able to compare the plasma-processing results obtained with the nanosecond pulse source with results of a slower pulse source.

The conventional pulse source consists of a high-voltage capacitor that is charged by a DC-source and discharged by a spark gap into a 50-Ω RG218 cable of 3 m [55]. A coupler is connected at the end of the cable to connect the pulse source to a high-temperature setup that we will not discuss in this paper. Integrated in this coupler are a capacitive voltage sensor and a Rogowski current sensor. Together with passive integrators connected at the wall of the EMC cabinet these sensors form a D-I (Differentiating-Integrating) system [58]. To conveniently make use of these sensors we designed an extension for this coupler to connect the corona-plasma reactor of Fig. 1 to the conventional nanosecond pulse source with a minimum of impedance mismatch.

Figure 4 shows examples of the voltage and current measured with these sensors (V_{reactor} and I_{reactor}) for two different voltage amplitudes. The rise time of the pulses is 5.7 ns and the pulse duration of the pulses from the conventional pulse source is

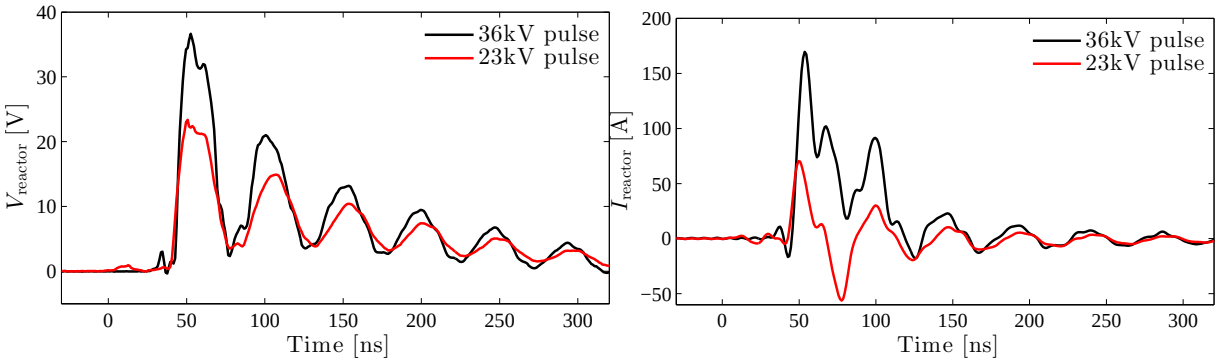

Figure 4: Example waveforms measured at the beginning of the corona-plasma reactor for two different output voltages of the conventional nanosecond pulse source. The figure shows (a) the reactor voltage and (b) the reactor current.

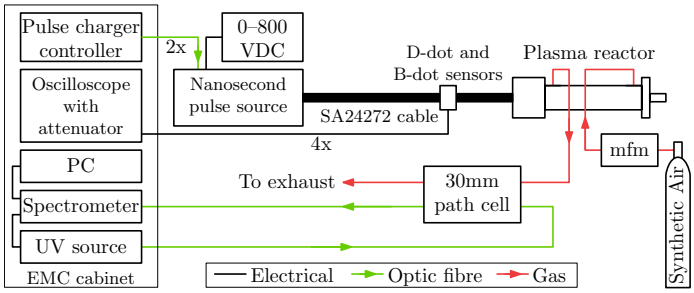

Figure 5: The total experimental setup for the ozone measurements. In the gas outlet of the reactor a 30-mm path cell is used for the UV spectrometer measurements to measure ozone concentrations.

22 ns. The variation of the output voltage amplitude is very stable (within ±2% of the average amplitude) because a triggered spark gap is used in this source. Furthermore, the reflections from the reactor are reapplied to the reactor in quick succession due to the short length of the RG218 cable.

2.4. UV-absorption spectrometry

In this paper we investigate two plasma processes: ozone generation and NO removal. In both processes, ozone is formed. In the NO experiments we measure the ozone with the FT-IR-method described in the next section. However, when we generate ozone in synthetic air (the first plasma process) we measure ozone with the UV-absorption-spectrometry method that we used in [50]. Figure 5 shows the experimental setup for this process when we use the nanosecond pulse source. The flow of synthetic air was set with a Bronkhorst MV-304 mass-flow meter ('mfm' in the figure).

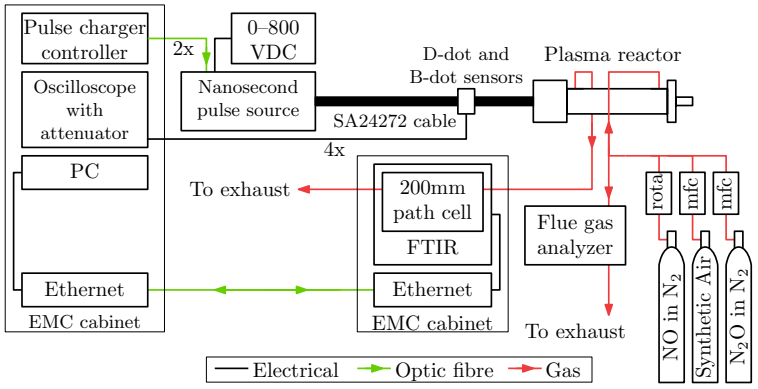

Figure 6: The total experimental setup for the NO-removal experiments. The nanosecond pulse source setup, the electrical diagnostics and the reactor are the same as in the ozone measurements. The UV-spectrometer is replaced by a FT-IR system which consists of a FT-IR spectrometer with a 200-mm long gas cell which is optically connected to a PC. The FT-IR setup is placed in its own EMC cabinet. Additionally, a flue gas analyser is added for NO-calibration and NO_2-calibration measurements.

2.5. FT-IR absorption spectrometry

In our experiments on NO removal we use FT-IR (Fourier Transform Infrared) absorption spectrometry to measure the significant compounds in these processes [59]. Figure 6 shows the total experimental setup for these measurements. We exchanged the UV-spectrometer setup for the FT-IR spectrometer setup, which consists of a Bruker Tensor 27 FT-IR Spectrometer (with a MCT 318/Z detector) in its own EMC cabinet. It measures the FT-IR spectra in the exhaust of the reactor in a 20-cm path cell.

Another addition to the setup is a Testo 350 XL flue-gas analyser. This system samples the gas at the inlet of the reactor to determine input NO and NO_2 concentrations. It is only used for calibration and to determine the initial concentration of NO in the gas supply and is decoupled during plasma operation.

The gas supply has been expanded compared to the ozone setup (and the synthetic air is now regulated with a Bronkhorst F-201AV mass-flow controller). The gas cylinder with N_2O (10000 ppm) in N_2 is only used for calibration and can be added to the gas supply with a Bronkhorst F-201AV mass-flow controller ('mfc' in the figure). The gas cylinder with NO (10000 ppm) in N_2 is used to supply the initial concentration of NO to synthetic air in all the NO-removal experiments and is added with a rotameter ('rota'). Furthermore, synthetic air is the bulk gas during the NO-removal experiments.

The compounds (that are relevant and significantly present in the FT-IR spectra) we measure for the NO-removal experiments are: NO, NO_2, N_2O, O_3, N_2O_5 and HNO_3. We measured all compounds quantitatively (apart from N_2O_5 and HNO_3, which were not calibrated and could only be measured qualitatively).

2.6. Yields

2.6.1. Ozone production The ozone-yield calculation we use for the experiments with the nanosecond pulse source is given by

$$G_{\mathrm{O_3}} = \frac{C_{\mathrm{O_3}} \times \mathrm{FW\,O_3} \times 3.6}{V_{\mathrm{m}}\varepsilon}, \tag{16}$$

where $G_{\mathrm{O_3}}$ is the ozone yield (in g·kWh^{-1}), $C_{\mathrm{O_3}}$ is the ozone production (in ppm), FW $\mathrm{O_3}$ is the formula weight of ozone (48.00 g·mol^{-1}), V_{m} is the molar volume (24.5 L·mole^{-1} at room temperature and atmospheric pressure) and ε is the energy density (in J·L^{-1}) which is defined as

$$\varepsilon = \frac{f_{\mathrm{rr}} E_{\mathrm{p}} \times 60}{F}, \tag{17}$$

where E_{p} is the total dissipated energy (in J) by the plasma generated by the nanosecond pulse source (see [50] for details) or the conventional pulse source, F is the gas flow (in slm) and f_{rr} is the repetition rate of the pulse source (in Hz).

2.6.2. NO removal We calculate the yield of the NO removal in the same way as the ozone-production yield, but without converting the amount of mole to grams. Therefore we obtain the NO-removal yield G_{NO} (in mol·kWh^{-1}) with

$$G_{\mathrm{NO}} = \frac{C_{\Delta\mathrm{NO}} \times 3.6}{V_{\mathrm{m}}\varepsilon}, \tag{18}$$

where $C_{\Delta\mathrm{NO}}$ is the amount of removed NO (in ppm).

Alternatively, we can define the energy cost W_{NO} (in eV per NO molecule removed) that is often used in literature as

$$W_{\mathrm{NO}} = \frac{V_{\mathrm{m}}\varepsilon \times 37.3}{C_{\Delta\mathrm{NO}} \times 3.6} = \frac{37.3}{G_{\mathrm{NO}}}. \tag{19}$$

3. Ozone production

In this section we describe the experiments of the first plasma-processing application: ozone generation.

3.1. Previous results with the nanosecond pulse source

Previous ozone measurements we performed during energy transfer efficiency experiments [50] showed that

- the ozone yield decreases with the energy density;
- the ozone yield slightly increases with the applied voltage at some settings;
- the ozone yield is higher for positive applied voltages;
- the pulse duration has no significant effect on the ozone yield;

The effect that a higher energy density decreases the ozone yield was also reported in [49, 8, 7, 24, 60, 12]. This effect is called *discharge poisoning* and happens when

ozone is generated in air. This process is the result of an increase in the concentration of NO_x and an increase in the gas temperature with energy density. Both of these effects promote the reaction of ozone with NO_x and consequently reduce the ozone concentration [7, 61, 8].

At first glance, the second observation is in contradiction with the first observation because a higher applied voltage increases the energy density. In some of the studies that we cited the ozone yield indeed decreased with the applied voltage [49, 12, 60], but in other studies the yields increased with the applied voltage [23, 22], just as in some of our experiments. Therefore, the effect that the voltage amplitude has on the ozone yield appears a specific effect for each reactor configuration and the consequent streamer phases (primary, or primary+secondary) at each applied voltage.

We know from our imaging experiments with the nanosecond pulse source [62] that the streamer velocity is higher for a higher applied voltage due to an increased enhanced electric field at the streamer head. This streamer head generates radicals needed for the ozone production, so as long as the streamer propagates, a higher voltage can increase the radical production.

We discuss the last two observation from the bullet list in the next parts.

3.2. Pulse duration

We saw in [50] that there was no significant effect of pulse duration on the ozone yield. Here we verify this observation by performing ozone yield measurements for eight different pulse durations (2–9 ns) at three different voltages for both polarities. Figure 7 shows the results of this measurement.

The results show some variation with pulse duration, but only very slightly. The ozone yields are slightly higher in the middle of the range of pulse durations and decrease when the pulse duration is increased further.

We know from our imaging experiments that the streamers in our corona-plasma reactor are mainly primary streamers [62]. Only somewhere in the range $\Delta t = 6$–9 ns streamers start to cross the gap from the high-voltage wire to the grounded outer cylinder at some points in the reactor at applied voltages of 25 kV and higher (an example, including streamer crossing, is shown in Fig. 8). Therefore, in general it holds for pulse durations up to 6 ns that an increase in pulse duration increases the volume of the reactor in which streamers are active (the "streamer volume"). Only when the voltage becomes higher, or the pulse duration longer, will the streamer volume stop increasing due to crossing streamers. For these pulse-source settings where the streamer volume stops increasing, the ozone yield appears to decrease. When the pulse duration increases even more at high voltages, the yield decreases further. Therefore, as long as the streamer volume can expand (by increasing the voltage or the pulse duration) the ozone yield is constant or even increases slightly, but when the plasma-volume expansion decreases, the ozone yield also decreases. However, we should note that all these changes in the ozone yield are very slight.

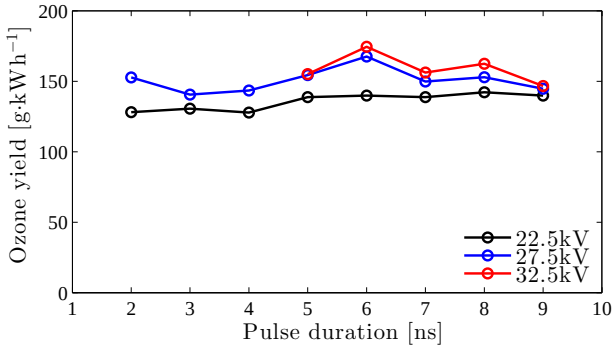

(a)

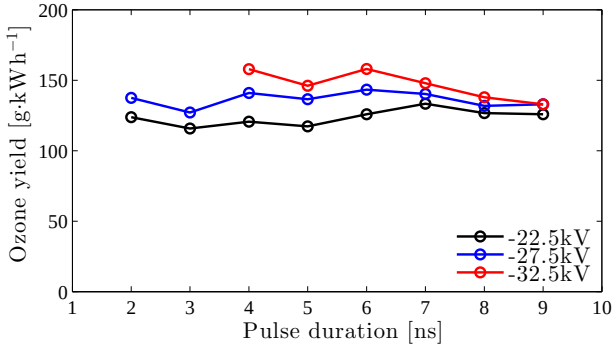

(b)

Figure 7: Ozone yields for different pulse source settings for 400-ps rise time (a) positive voltages and (b) negative voltages for $f_{\mathrm{rr}} = 100\,\mathrm{Hz}$ and $F = 5\,\mathrm{slm}$.

From the results in [62] we know that we have no visible secondary-streamer phase when the streamers have crossed the gap, but there will likely be secondary effects such as the onset of secondary streamers that are not visible in the ICCD-imaging or the heating of the streamer channel. Therefore, when the streamer volume stops increasing, secondary-streamer effects could increase.

Van Heesch *et al.* [9] and Eichwald *et al.* [63] show that the oxygen-radical energy yield is lower in the secondary-streamer phase as compared to the primary-streamer phase. If the streamers in our plasma cross the gap, secondary-streamer effects might start to occur and according to Van Heesch *et al.* and Eichwald *et al.* the oxygen-radical energy yield would consequently decrease. This would explain why the ozone yields decrease in our plasma when the streamer volume is unable to expand any further. However, Ono *et al.* [64] and Komuro *et al.* [65] show that atomic oxygen is mainly (energy efficiently) produced in the secondary-streamer phase, which is in contradiction with the findings of Van Heesch *et al.*. Komuro *et al.* claim that the fact that Van Heesch *et al.* used moist air instead of dry air (as Komuro *et al.* and Ono *et al.* use) might be a possible reason for this contradiction. Furthermore, they note that in the discharge of Eichwald *et al.* the secondary streamer is short compared to the primary streamer (where their own streamers are more than half of the length of the primary streamer) and that therefore the oxygen radical yield of the primary and secondary streamer are

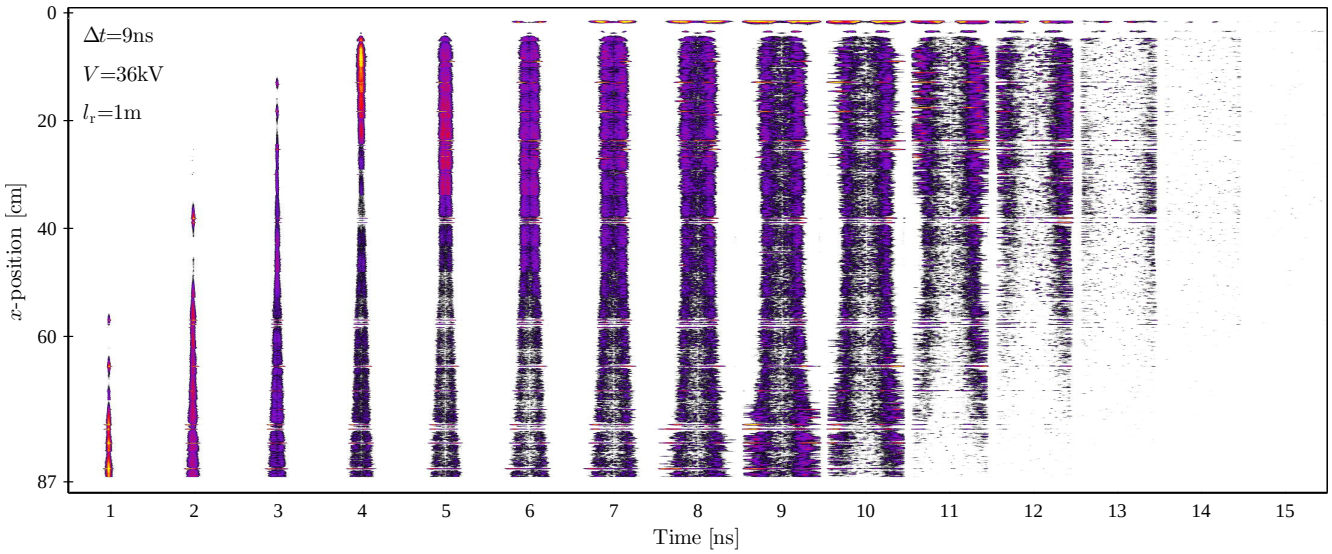

Figure 8: Streamer development in time for a 400-ps rise time, 9-ns positive pulse in a 1-m reactor. The exposure time is 1 ns for all images and each image is the average of 20 photos at each position. The bottom of each subimage is the input of the plasma reactor and the top is the end of the reactor (where bright discharges appear at the wire-tightening mechanism). Only primary streamers are visible for the duration of the discharge. More details (on the experimental setup, ICCD images, SPICE simulations and analysis) can be found in [57] and [62]. Reproduced from [62].

much closer. In our plasma the secondary streamers likely hardly exist, and therefore the findings of Eichwald *et al.* are more applicable to our plasma. The pulses used by Van Heesch *et al.* are also significantly shorter than used by Komuro *et al.*, Ono *et al.* and Eichwald *et al.*. We used even shorter pulses with a much shorter rise time. Without using significantly longer pulses (with the same short rise time as the pulses from our nanosecond pulse source) it is not possible to draw concrete conclusions from our results with respect to radical generation in the primary and secondary-streamer phase, but our results might be explained from a higher oxygen-radical formation energy efficiency in primary streamers, which would be in agreement with Van Heesch *et al.* and Eichwald *et al.*.

A second effect that we have to consider is that as the streamer approaches the grounded electrode, the electric field at the streamer head increases significantly due to the close proximity of the ground electrode. Therefore, just before the streamers cross the gap in the electrode, the radical formation will be enhanced. Consequently, just before the streamer volume stops decreasing, there is a phase in which radical production is enhanced.

3.3. Pulse polarity

In [50] we found that applying negative pulses resulted in a higher energy transfer (or better "matching") of the pulse source to the reactor than when we use positive pulses, but that the associated ozone yield was lower. In [62] we then discovered the presence of thick streamers on the tightening mechanism of the reactor that likely dissipate a significant amount of energy (shown at the top of the images in Fig. 8). Due to this loss in energy, the streamer development in the reactor was affected in such a way that the total streamer volume was smaller than when positive pulses were used. Since the thick streamers at the end of the reactor will exist for a large part in the secondary-streamer phase, consume a significant amount of energy and result in a smaller streamer volume, the ozone yield for the negative pulses will be lower. This is in contradiction with some other studies, which found higher ozone yields for negative pulses (e.g. [9, 21]). Here we will analyse the results with a different method to try to understand this discrepancy.

With the ICCD imaging setup of [57] it is possible to follow the streamer development in the reactor on a very short time scale as a function of time and position in the reactor. It is therefore possible to calculate the total streamer volume for each time step from the streamer width, the streamer length and the number of streamers. If we would then calculate the total streamer volume for a number of applied voltages and pulse durations at both polarities, we could relate the measured ozone concentrations to the calculated streamer volume and might arrive at an ozone yield per streamer volume unit. Unfortunately, this requires the data from a large amount of experiments, which we do not have at this moment. However, with the data we have from [62] we can relate the ozone concentrations to the average streamer lengths at different applied voltages and pulse durations for both polarities.

In [62] we showed the average maximum streamer lengths as a function of the position in the reactor for different applied voltages and pulse durations for both polarities. If we take the average of these streamer lengths $\widetilde{s_{\mathrm{x}}}$ (in mm) for each experimental setting, we can compare these average streamer lengths to the ozone production at the same settings in the current paper by dividing the ozone production with a constant α. Here, α has the unit ppm·mm^{-1} and is selected in such a way that the results have a good fit. Figure 9 shows the results if we perform this fitting for both polarities.

The available data is not extensive, but the results show a reasonable fit between the scaled ozone production and the average streamer length in the reactor. This indicates that the plasma generated with the short-rise time pulses might have an inherent parameter that relates the amount of ozone it produces to the dimensions of the plasma in the primary-streamer phase.

For the results of Fig. 9 the parameters α_{p} and α_{n} are the α-values for the positive and negative results respectively and are 155 ppm·mm^{-1} and 170 ppm·mm^{-1} respectively. These values indicate that the negative plasma is more effective per mm of average streamer length in generating ozone. We have no way of relating this to

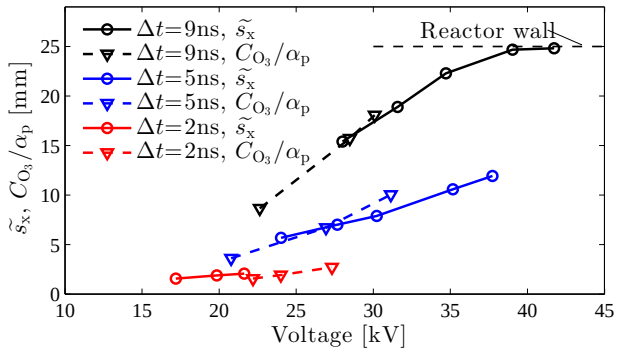

(a)

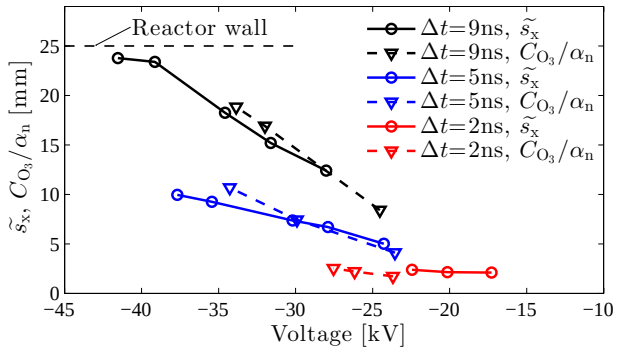

(b)

Figure 9: A comparison between scaled ozone concentrations (C_{O_3}/α) and the average streamer length ($\widetilde{s_x}$) in the reactor for (a) positive and (b) negative polarities. The α-parameter is the scaling parameter for the ozone concentrations and is chosen such that the results show a good fit. The α-parameter is different for both polarities and is higher for the negative pulses.

the dissipated plasma energy because we have no information on the energy dissipated by the thick streamers, but it is a strong indication that the negative streamers in the main plasma are actually more effective at generating ozone when compared to positive streamers. Consequently, this result is in agreement with what other researchers found.

3.4. Rise time

In [5] we showed how we can change the rise time of our nanosecond pulses by introducing capacitors in the plasma reactor. Subsequently, we showed that the rise time has a significant effect on the streamer propagation: when the rise time increases, the streamers propagate slower and less far [62]. Consequently, the streamer volume in the reactor is significantly smaller. At the same time, the dissipated energy is also lower, but not significantly lower. Now we measured the ozone production at the same rise times and arrive at the results of Fig. 10a. The results show that shorter the rise times result in higher the ozone yields. If we consider that the main source of radicals required for ozone production is the enhanced electric field at the streamer head (resulting in the

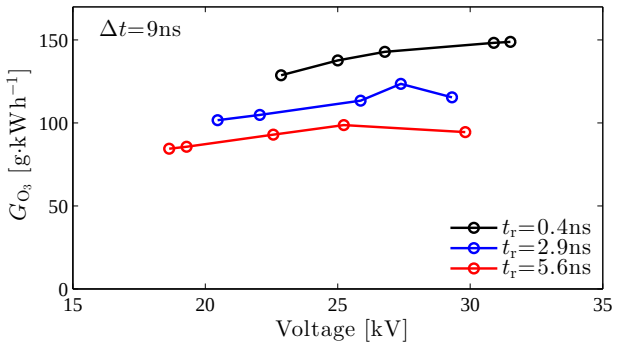

(a)

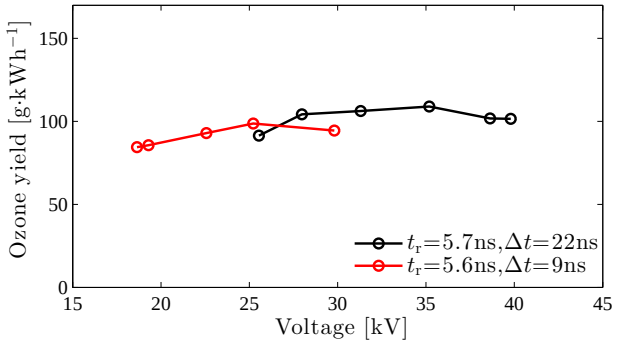

(b)

Figure 10: Ozone yields for pulses with different rise times. In (a) we used the pulses from the nanosecond pulse source with 9-ns pulse duration with three different rise times for $f_{rr} = 20\,\text{Hz}$ and $F = 2\,\text{slm}$. In (b) we compared the ozone yield of the 5.6-ns rise time pulse of the nanosecond pulse source of (a) with the yield of the conventional pulse source. The experimental settings for the measurements with the conventional pulse source were the same as for (a).

high-energetic electrons required for e.g. (1), (3) and (4)) and that a longer rise time results in a smaller streamer volume, then the result that a longer rise time results in a lower ozone yield in our reactor is not surprising.

In addition to the nanosecond pulse source we used the conventional pulse source that we introduced in Section 2.3 to perform ozone production experiments. The pulses from this pulse source have a similar rise time as the longest rise time from our nanosecond pulse source, but with a longer pulse duration of 22 ns. Figure 10b shows the comparison between the results of the two different pulse sources. We see that the ozone yields are very similar, which is further proof that the rise time is a very important parameter for the ozone yield for these short pulses. We could argue that at a pulse duration of 22 ns the streamers could enter the secondary-streamer phase, but we have no ICCD-imaging results with the conventional pulse source. However, we know from [62] that the streamers generated with the 5.6-ns rise time pulses are much slower than the 0.4-ns rise time pulses. Therefore at 22 ns the streamers might just cross the gap and will likely be primary streamers still. Consequently, their behaviour should be

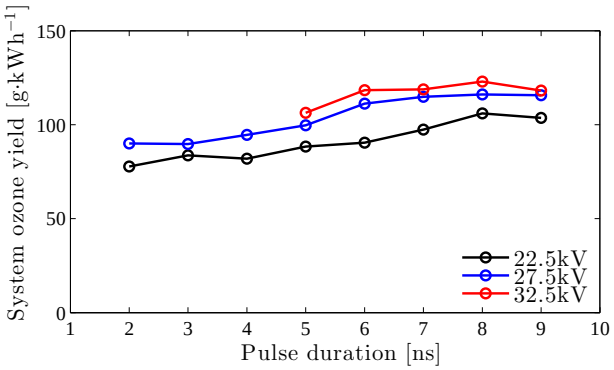

(a)

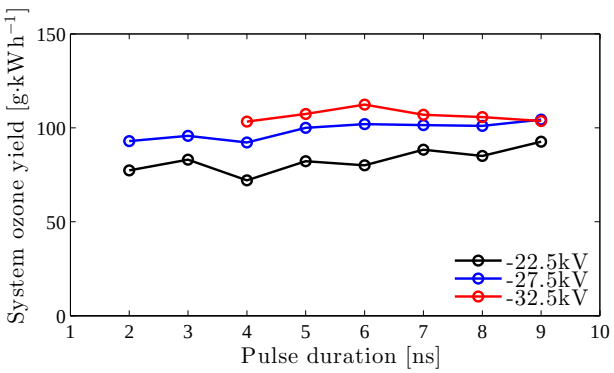

(b)

Figure 11: The total system yield for ozone production for 400-ps rise time (a) positive voltages and (b) negative voltages. The ozone yield results of Fig. 7 were multiplied by the matching of the pulse source to the reactor at those settings to obtain the system yield. The results show that using positive, long pulses at a high voltage results in the highest system yield.

similar to the streamers generated with the 5.6-ns rise time pulse from the nanosecond pulse source and Fig. 10b confirms this. It even shows the slight trend that the ozone yield increases with the applied voltage.

In conclusion, the rise time of the applied pulses has a very significant effect on the ozone yield. In future experiments, the use of longer pulses with the same short rise time as the fastest pulse from our nanosecond pulse source would be very useful to determine what the most important parameter for ozone production is — rise time or pulse duration — when the streamers also exist for a significant part in the secondary-streamer phase.

3.5. Optimal parameters for ozone production

After the experiments on ozone production in this paper, the question is: what is the optimal pulse source setting to produce ozone (and therefore atomic oxygen)?

Obviously, it is beneficial to have a high ozone yield, but if the energy transfer of

the pulse source to the reactor at that particular setting is low, the total yield of the reactor as an entire system can still be low. Therefore we require good matching and a high ozone yield simultaneously. We calculate the system yield with

$$\text{System yield} = G_{O_3} \times \eta_{\text{tot}}, \tag{20}$$

where η_{tot} is the total matching of the pulse source to the reactor.

The results of this section showed that the rise time has to be as short as possible for the highest yield. Furthermore, we measured that the matching of the long-rise time pulses is lower, so we only calculate the system yield for the shortest rise time pulses. Figure 11 shows this system yield as a function of the pulse duration and voltage amplitude for the short-rise time pulses.

The nearly constant ozone yield, coupled with the increased matching for longer pulses, results in a system yield that increases with the pulse duration. Furthermore, due to better matching and a high ozone yield at higher applied voltages, the system yield increases with the voltage as well. If we then consider that the longest pulses and the highest voltages generate the highest ozone concentration, the optimal pulse source parameters for ozone generation in dry synthetic air are 8–9-ns positive pulses at the highest voltage we used.

4. NO removal

In this section we present the results of the NO-removal experiments.

4.1. Pulse polarity and initial concentration

Just as with the ozone-production experiments, we start by varying the pulse duration, pulse amplitude and pulse polarity of the applied pulses and study the effect on the plasma process. In this first part we begin with the effect of the pulse polarity. We used three different pulse durations (2 ns, 5 ns and 9 ns) at three different voltages for both amplitudes. We used an initial concentration of 220 ppm NO in synthetic air for these measurements. This value is in the range of 200-300 ppm that is often used by other researchers and gives a good approximation of a typical flue-gas composition. Figure 12a and Fig. 12b show the results of the FT-IR measurements as a function of the energy density. We first focus on the formed compounds.

The results of the experiment show that the concentration of the various compounds is mainly the result of the energy density and not so much the result of different pulse durations and voltages.

When the energy density increases, the concentration of NO decreases and the concentration of NO_2 increases through reactions (5)–(8). Meanwhile NO_2 can be converted to by-products N_2O and N_2O_5‖ through reactions (9)–(11), but as long as

‖ In this discussion, keep in mind that the N_2O_5 results are not calibrated. To obtain the concentrations in the figures, we multiplied the absorbance in the N_2O_5 range with an arbitrary constant number. Therefore, the N_2O_5 concentrations in the figures could be much lower than they are represented.

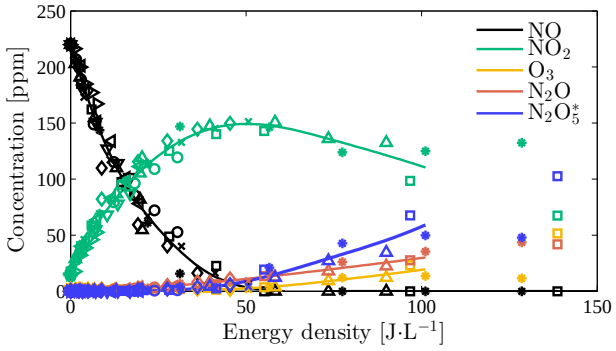

(a)

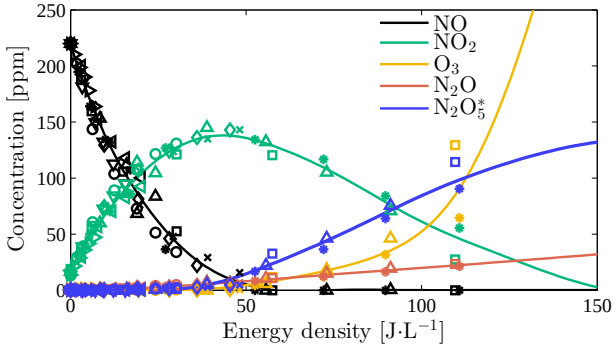

(b)

Figure 12: The results of the FT-IR measurements for 400-ps rise time (a) positive pulses and (b) negative pulses for the NO-removal experiments at different applied voltages and pulse durations at a flow of 4 slm. The energy density is changed with the pulse repetition rate. The initial concentration of 220 ppm of NO is converted to NO_2, N_2O, O_3 and N_2O_5 by the plasma. The figure shows the raw values (the markers) and the fitted values. The fitted lines were fitted with the inclusion of raw results up to 250 $J{\cdot}L^{-1}$ for the negative pulses and up to 100 $J{\cdot}L^{-1}$ for the positive pulses (at higher energy densities some experiments showed unexpected results). The markers represent measurements with a pulse duration and applied voltage (positive and negative amplitude respectively) of: ($\circ$) 2 ns (29 kV and -31 kV), (∇) 2 ns (23 kV and -24 kV), ($\triangleright$) 2 ns (17 kV and -15 kV), (Δ) 5 ns (32 kV and -33 kV), ($\times$) 5 ns (24 kV and -25 kV), ($\triangleleft$) 5 ns (16 kV and -17 kV), ($\square$) 9 ns (37 kV and -38 kV), ($*$) 9 ns (30 kV and -29 kV) and ($\Diamond$) 9 ns (19 kV and -20 kV). *Note that the N_2O_5 concentration is not calibrated.

NO is present in the reactor the contribution of these reactions is minor. Once the NO concentration becomes low (at around 40–50 $J{\cdot}L^{-1}$) the production of NO_2 from NO decreases and reactions (9)–(11) become dominant in the formation of by-products. Furthermore, once all NO is removed from the gas and the NO_2 concentration becomes low, O_3 is not lost anymore to reaction (8) and its concentration can increase significantly (as we see for the negative-polarity results).

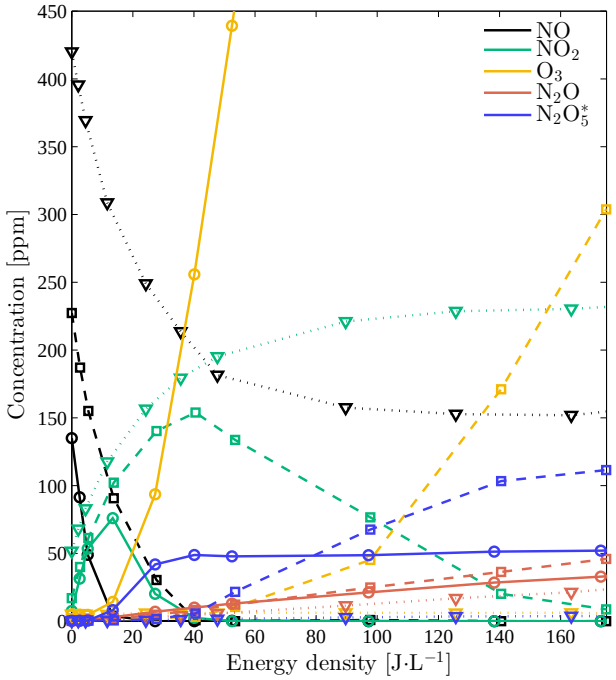

Figure 13: The results of FT-IR measurements for 400-ps rise time, 9-ns, 31-kV positive pulses for three different initial concentrations of NO: 135 ppm (solid line), 225 ppm (dashed line) and 420 ppm (dotted line) at a flow of 4 slm. *Note that the N_2O_5 concentration is not calibrated.

4.1.1. Initial NO concentration Before we compare the results of both polarities, we first show results of an experiment in which we varied the initial concentration of NO (135 ppm, 225 ppm and 420 ppm) to see the effect this has on the formed compounds. We used 9-ns, 31-kV, positive pulses for these experiments and varied the pulse repetition rate to increase the energy density. Figure 13 shows the results.

The first observation from the results is that for the lowest two concentrations, all NO is converted, but that for an initial concentration of 420 ppm the NO concentration stabilises at a non-zero concentration. Mizuno *et al.* encountered a similar effect for high initial NO concentrations and attributed the effect to the destruction of ozone at high energy densities [30]. A lower ozone concentration would consequently reduce the conversion of NO to NO_2 and of NO_2 to NO_3 (and consequently to N_2O_5) through reactions (8) and (10)–(11) respectively. However, we can see from the ozone concentrations of the 135-ppm and 225-ppm results that the ozone concentration still increases at high energy densities, so the energy density is not yet high enough to decrease the ozone concentrations significantly. Furthermore, the N_2O_5 concentration also still increases, indicating that in our process ozone is still important through reactions (10)–(11).

An important clue to explain our results is the concentration of N_2O. For N_2O to form, NO_2 and atomic nitrogen have to be available for reaction (9). According to the results, the concentrations of NO and NO_2 are zero for the 135-ppm results at

high energy densities, yet the N_2O concentrations steadily increases with the energy density, indicating the presence of NO_2. Therefore, the NO production reaction (14) has to play an important role. The constant production of new NO will result in new NO_2, which will consequently be converted to N_2O. (This also shows that for these experiments, reaction (9) is preferred over (10) because the N_2O_5 concentration does not increase significantly at higher energy densities and only increases when the NO_2 concentrations are high.) Therefore, from the 135-ppm results we can conclude that besides NO removal, the plasma also constantly produces new NO and the subsequent by-products. This was also observed by Beckers *et al.* for low-level NO_x removal [28].

At an initial NO concentration of 225 pm all NO can be removed, but it already takes a considerably higher energy density to remove all NO_2 (as compared to the 135-ppm results), indicating that the production of NO by the plasma, and back reactions from NO_2 to NO, such as (15), start to dominate. At an initial NO concentration of 420 ppm NO can not be completely removed anymore and appears to converge to an end value. The same is true for NO_2 and it therefore appears that the production of NO from NO_2 through (15) and vice versa through (5), (7) and/or (8) dominates the process at high energy densities. Consequently, the production of the other by-products is almost completely suppressed. The production of some N_2O indicates that some atomic nitrogen are used to convert NO_2 into N_2O, but that most NO_2 and atomic nitrogen are involved in other reactions.

From the results it appears that the nanosecond pulsed plasma is unable to remove high NO concentrations. Fortunately, there are methods available to overcome this issue. For instance, the addition of C_2H_4 to the plasma greatly enhances the NO removal due to the formation of other types of radicals in the plasma [30, 66]. We did not perform experiments with additives, so results of these type of experiments will be left for future work. Also the addition of H_2O will reduce the NO_2 concentrations and will consequently result in more NO removal at higher initial concentrations as we will see later and was also mentioned in [30].

Finally, we look at the NO-removal yield for the experiments with different initial NO concentrations. Figure 14 shows these results. If we consider that at higher initial concentrations the production of NO and the interaction with NO_2 increases, it is not surprising to see the highest NO-removal yield for the lowest initial concentration. Furthermore, the results show very high yields at 50 percent removal for the 135-ppm concentration of 2.5 mol·kWh^{-1} (or 14.9 eV per NO molecule) and even for the 225-ppm results the yields are very high at around 1.75 mol·kWh^{-1} (or 21.3 eV per NO molecule).

4.1.2. Polarity In Fig. 15 we compare the fitted concentrations of the compounds in Fig. 12a and Fig. 12b of the positive and negative polarity pulses. The differences in NO removal are not significant and indicate a slightly better result for positive pulses. If we consider that the results of the ozone generation experiments showed that the ozone yields were higher for positive pulses, the NO-removal results are surprising. For ozone generation a higher amount of atomic oxygen produces more ozone.

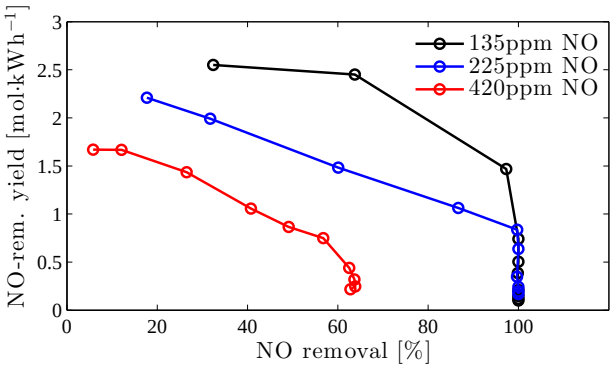

Figure 14: The NO-removal yields as a function of the amount of removed NO for the results of Fig. 13. The results show that the yield decreases when the initial NO concentration increases.

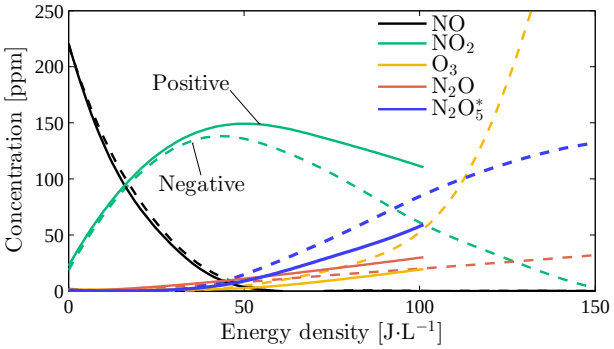

Figure 15: The fitted results of Fig. 12 for the positive pulses (solid line) and the negative pulses (dashed line). The NO removal is very similar for both polarities, but the by-product concentrations differ slightly.

Furthermore, excited nitrogen species produced in the primary-streamer phase (which is more pronounced for the positive pulses) result in a further increase in atomic oxygen [47, Section 2.5]. Therefore, we expected the NO-removal to be more efficient for positive pulses, because one of the important NO-removal reactions is the oxidation of NO through (5), which requires atomic oxygen. It therefore appears that for positive pulses the production of NO through (14) (and the back conversion of NO_2 to NO) is more pronounced than for negative pulses, which consequently keeps the NO concentrations higher than expected. Likewise, the NO_2 concentrations are higher. In fact, if we compare the positive results with the negative results, the results are very similar to when we compare the 225-ppm results with the 135-ppm results in Fig. 13 (only less pronounced).

For the production of NO through reaction (14), atomic nitrogen is required. Therefore, if the production of NO by the plasma is more pronounced for positive pulses, it is likely that more atomic nitrogen is produced for the positive pulses. Furthermore, the production of N_2O through (9) also requires atomic nitrogen and is also higher for positive pulses. The generation of atomic nitrogen requires higher electron energies

than atomic oxygen as we see from reactions (1) and (4) and because primary streamers produce electrons with a higher energy than secondary streamers, more atomic nitrogen will be produced in the primary streamers. With our previous conclusion that the primary-streamer phase is slightly more pronounced for positive pulses, this could explain the small differences in polarities: for positive pulses we have more atomic nitrogen and therefore a higher production of NO and N_2O. That we did not see these effects with the ozone-generation process is that according to Fig. 13 ozone production is not influenced much if the initial concentration of NO and NO_2 are low (for instance above $50\,J{\cdot}L^{-1}$ for the 135-ppm results). Only at very high energy densities will the effects of NO and NO_2 become significant [7, 61, 8]. We see this effect in [50, Fig. 18], where we observed that the positive ozone yields decrease more significantly with the energy density than the negative yields, which can again be explained with the results from the current paper.

4.2. Pulse duration and voltage amplitude

In the ozone-generation measurements of Section 3 we showed that the ozone yield increased slightly with the pulse duration, increased more significantly with the voltage and that these effects diminish at the longest pulse durations (6–9 ns). Furthermore, the ozone yields were lower for negative pulses. Figure 16 shows the NO-removal yields as a function of the amount of NO removed for different voltages and pulse durations. The results are listed below and are very similar to the observations on ozone yields of the ozone-generation experiments of Section 3.

- On average the NO-removal yields are slightly lower for negative pulses, but the difference is not as pronounced as with the ozone-generation experiments.
- The NO-removal yield increases with the applied voltage. This effect seems larger than with the ozone-generation experiments, but we have to keep in mind that the differences between the lowest and highest applied voltages are larger for the NO-removal experiments.
- At longer pulse durations the differences in NO-removal yields are smaller between the different applied voltages at that pulse duration.
- The NO-removal yield increases slightly with the pulse duration, but are very similar when the same voltage amplitudes are used.

These general observations show that there are slight differences in the yields between the ozone-generation experiments and the NO-removal experiments. However, while the governing reactions are very similar, one process is a generation process and the other a removal process. In the latter, the amount of remaining pollution significantly influences the plasma process (as we saw in the previous part) and therefore the yields. A direct comparison between the two processes can therefore not be made.

Some of the observations on the NO-removal yields can again be explained from the imaging results. A lower voltage reduces the electric field enhancement at the tip of the streamer and therefore the radical generation and the streamer velocity

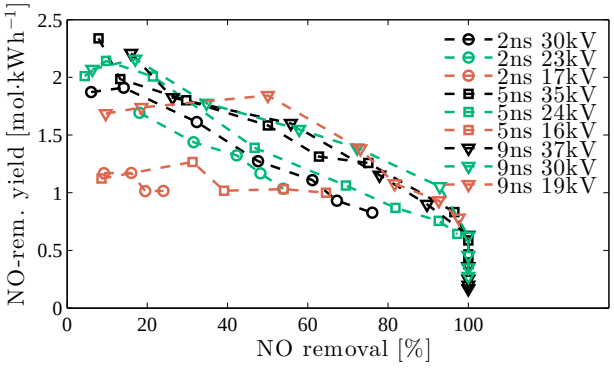

(a)

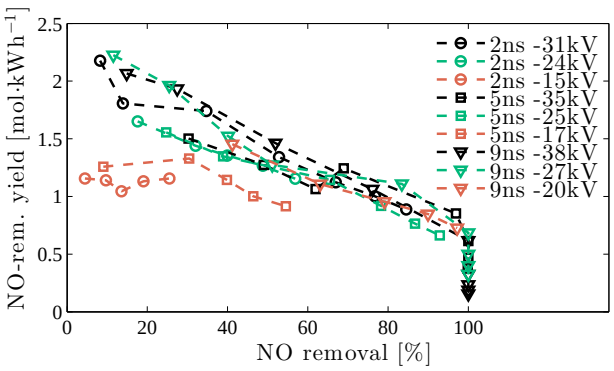

(b)

Figure 16: The NO-removal yields for different pulse durations and applied voltages for 400-ps rise time (a) positive pulses and (b) negative pulses for the results of Fig. 12 (220 ppm initial concentration) as a function of the percentage of the removed NO.

(and consequently the streamer volume). The energy that the streamers dissipate will consequently also be lower, but that the net result is a lower radical-generation yield seems likely. For short pulse durations, the applied voltage can increase significantly before the streamers cross the gap at these short durations. Only the ratio of radical formation in the primary streamer to the dissipated energy by the streamers then influences the NO-removal yield. From the results we see for the 2-ns results that an increased voltage increases the NO-removal yield. To a lesser extent, this is also true for the 5-ns measurements, but for the 9-ns measurements this is not true anymore. Here the yields are not very dependent on the applied voltage. If we again consider that for the 5-ns and 9-ns pulses the streamers can cross the gap in the reactor at some positions, and that this number of positions increases with the applied voltage, then radicals are formed partly after the primary-streamer phase. Furthermore, the energy dissipation by the plasma still increases with the pulse duration and applied voltage, so the NO-removal yield will consequently not increase anymore.

The analysis of the results is further complicated because the differences in NO-removal yields between various settings is small. Just like we concluded in the ozone-generation section, it would be beneficial to have the use of longer pulses (or a higher

voltage) with the same short rise time to be able to comment further on the effect of the secondary-streamer phase and to see if the similarities between the ozone-generation experiments and the NO-removal experiments still hold, or that they start to deviate. For instance, for longer pulses Fujiwara *et al.* and Kakuta *et al.* already showed that a long pulse duration decreases the NO-removal yield as compared to shorter pulses with the same rise time [13, 14].

Finally, we observe that at 50 percent NO removal we obtained a NO-removal yield of around 1.75 mol·kWh^{-1} (which corresponds to a cost of 21 eV per NO molecule). This yield is very high compared to other studies and might even be increased further by finding an optimum process temperature [25], by adding hydrocarbons into the gas stream [30] or by an indirect method where ozone is generated with the plasma and is then added to a gas stream containing NO [21].

4.3. Rise time

In the ozone-generation measurements of Section 3 we showed that the ozone yield decreased significantly when we used pulses with a longer rise time and we expect the same behaviour for the NO-removal experiments. Figure 17a confirms this expectation.

In Fig. 17b we compare the results of the 5.6-ns rise time pulse from the nanosecond pulse source with the results of the 5.7-ns rise time pulse of the conventional pulse source. Just as with the ozone-generation experiments, the results are very similar, again indicating that the rise time is a very important parameter for the plasma-processing yields.

4.4. H_2O addition

As a last experiment we used compressed ambient air with 4500 ($\pm$ 1500) ppm of H_2O and performed NO-removal measurements . Figure 18a compares the results of these measurements to NO-removal measurements with dry synthetic air (which still contains up to 10 ppm of H_2O). The effect of the H_2O is that reaction (13) becomes important. As a result, NO_2 is used that would be used for the generation of N_2O and N_2O_5 (through NO_3) if no H_2O was present. Therefore, the concentrations of NO_2, N_2O and N_2O_5 are lower when H_2O is added. Likewise, the concentration of HNO_3 is higher until all NO_2 is used.

If we look at the NO-removal yields in Fig. 18b we see that the addition of H_2O slightly lowers the NO-removal yield. This is because of the energy that is used for OH-radical generation and would otherwise have been used to generate atomic oxygen that could be used for the oxidation of NO through (5). Likewise, less energy is available for the generation of atomic nitrogen that could reduce NO through (6).

This experiment shows that by using moist air, less by-products are formed at the cost of an increased HNO_3 concentration. However, HNO_3 can be removed from the gas stream by conventional means.

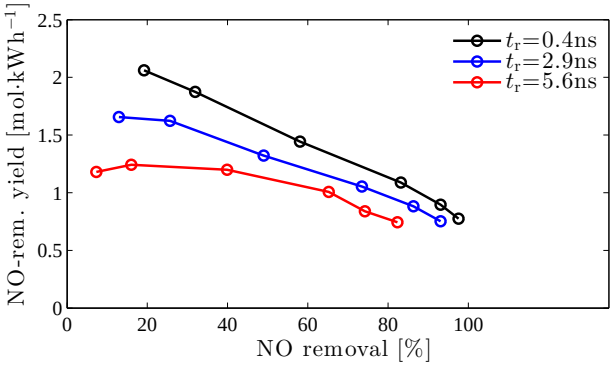

(a)

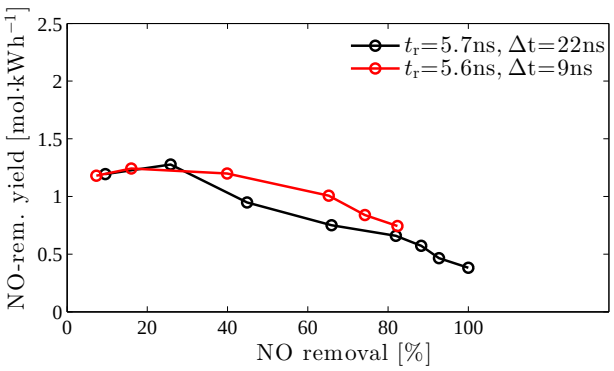

(b)

Figure 17: NO-removal yields for different rise-time pulses. In (a) all pulses were the 9-ns pulses from the nanosecond pulse source with a 30-kV amplitude and different rise times. The gas flow was 2 slm of synthetic air with 220 ppm NO. In (b) the NO-removal yields for the 5.6-ns rise time pulses from the nanosecond pulse source (same experimental conditions as (a)) are compared with NO-removal yields for the 5.7-ns rise time pulse from the conventional pulse source (38-kV pulses at $F = 2$ slm).

4.5. Optimal parameters for NO removal

Just as with the ozone-generation experiments we can calculate the total system yield with

$$\text{System yield} = G_{NO} \times \eta_{\text{tot}}. \tag{21}$$

Figure 19 shows the system yield for the NO-removal experiments. Due to the better matching at longer pulse durations and higher voltages, as well as the higher NO-removal yields at longer pulse durations and higher voltages, the system yields are consequently highest for the longest pulses and the highest voltages. Therefore, the optimal pulse source parameters for NO-removal are the longest available pulses of our nanosecond pulse source at the highest voltage. Furthermore, for a lower by-product formation of NO_2 and N_2O, a negative polarity is preferred. However, if a lower ozone concentration and a lower N_2O_5 concentration is required, positive pulses are preferred.

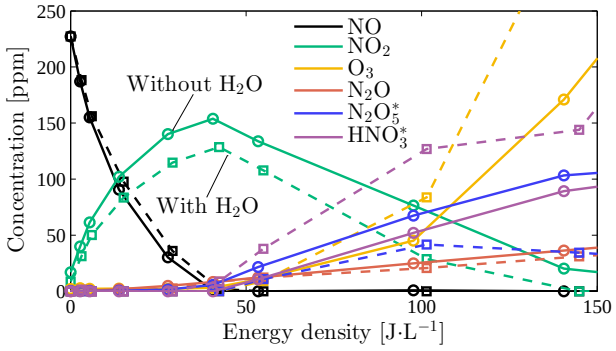

(a)

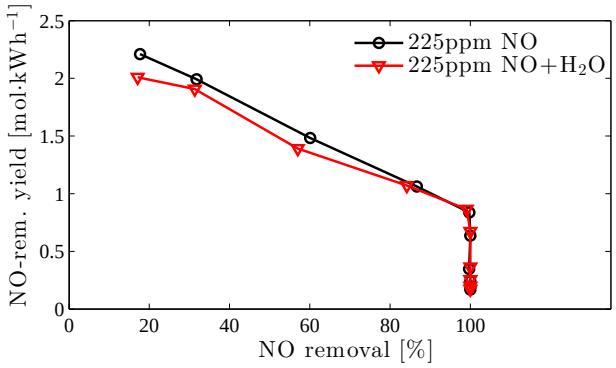

(b)

Figure 18: NO-removal experiments with and without added H_2O. In (a) the various compounds are shown for a gas stream with water vapour (dashed line) and without water vapour (solid line) for an initial concentration of 225 ppm of NO for $F = 4$ slm). The pulses were 400-ps rise time, 9-ns, 35-kV positive pulses. In (b) we compare the NO-removal yields for both experiments. *Note that the N_2O_5 and HNO_3 concentrations are not calibrated.

Table 1: Influence of pulse parameters on plasma yields.

	Ozone generation	NO removal
Amplitude ↑	+	+
Rise time ↓	++	++
Pulse duration ↑	+/-	+
Positive polarity	+	0

5. Summary and conclusions

In this paper we applied our nanosecond pulse technology to two plasma processes: ozone generation and NO removal. Above all, we showed that the nanosecond pulses produce an efficient plasma for ozone generation and NO removal.

The most important findings are listed below.

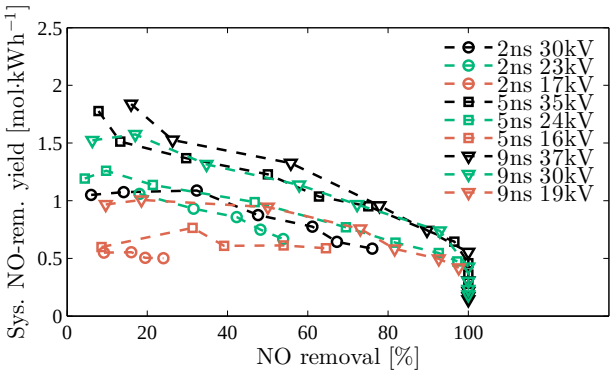

(a)

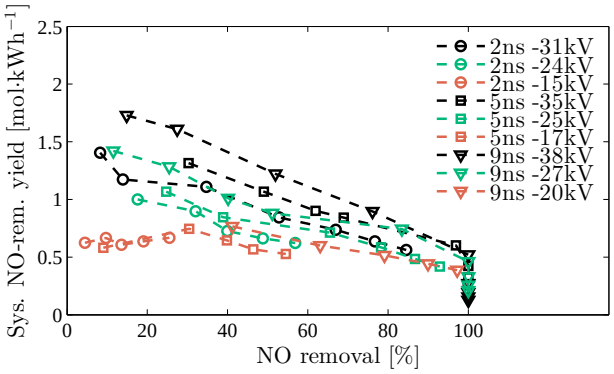

(b)

Figure 19: The total system yield for NO-removal for 400-ps rise time (a) positive voltages and (b) negative voltages. The NO-removal yield results of Fig. 16 were multiplied by the matching of the pulse source to the reactor at those settings to obtain the system yield. The results show that using long pulses at a high voltage results in the highest system yield.

Table 2: Influence of pulse parameters on system yields.

	Ozone generation	NO removal
Amplitude ↑	+	++
Rise time ↓	+++	+++
Pulse duration ↑	+	++
Positive polarity	+	0

- The maximum obtained ozone yields were around 175 g·kWh^{-1} in synthetic air which is high compared to other pulsed corona plasmas.
- NO can be removed very efficiently from synthetic air with yields as high as 2.5 mol·kWh^{-1} (or 14.9 eV per NO molecule) for a 135-ppm initial NO concentration at 50 percent removal and even for the 225-ppm results the yields are very high at around 1.75 mol·kWh^{-1} (or 21.3 eV per NO molecule) at 50 percent removal.

However, for higher concentrations the yields decrease significantly. From an analysis of all the by-products formed in the plasma with NO, we could conclude that due to the production of NO by the plasma, at high NO concentrations the NO concentration will be in equilibrium with the NO_2 concentration at high energy densities, inhibiting further removal of NO. Solutions to this problem were suggested.

- The streamer volume and the consequent streamer phase (primary/secondary) appear to influence the ozone yield slightly. When the pulse duration and/or the applied voltage increases, the electric field in the reactor increases and the streamer volume increases until streamers start to cross the gap in the reactor. As long as the streamer volume can increase, the ozone yield increases slightly with the pulse duration and more significantly with the applied voltage. When the pulse duration and/or the applied voltage is increased further, the increase in streamer volume slows and finally stops. At this point secondary-streamer effects can become important and the ozone yields start to decrease. For the NO removal, the results are similar and also dependent on the streamer volume, but the pulse-duration effect is more pronounced, even though the differences in yield between the various settings are small.
- Increasing the rise time of the applied pulses decreases the ozone yield and NO removal yield due to a much smaller streamer volume that is generated with only slightly less energy. A longer pulse from a conventional pulses source, with a similar rise time as a short pulse from the nanosecond pulse source, results in a similar yields, indicating that as long as there are no secondary-streamer effects, the yields appear to be determined by the rise time rather than the pulse duration.
- The dependency of pulse parameters on the yields is summed up in Table 1 and 2, which show the plasma yields and the system yields of the two processes respectively. The '+'-symbols indicate how strong the yields increase with the change in the stated parameter, the '+/-'-symbol indicates that the yield can either decrease or increase, depending on other settings and a '0' indicates that the yields do not significantly depend on that parameter.
- The optimal parameters for ozone production and NO removal are a long pulse duration at the highest, positive voltage if we include the energy transfer of the pulse source to the plasma. In addition, for NO removal, depending on which by-product is preferred, negative pulses (more ozone and N_2O_5) or positive pulses (more N_2O and NO_2) can be used.

Acknowledgements

This work was supported by the Dutch Technology Foundation STW under contract number 10751.

References

[1] Kim H H 2004 *Plasma Processes and Polymers* **1** 91–110 ISSN 1612-8869

[2] Kogelschatz U 2003 *Plasma chemistry and plasma processing* **23** 1–46

[3] Fridman A, Chirokov A and Gutsol A 2005 *Journal of Physics D: Applied Physics* **38** R1

[4] Samukawa S, Hori M, Rauf S, Tachibana K, Bruggeman P, Kroesen G, Whitehead J C, Murphy A B, Gutsol A F, Starikovskaia S, Kortshagen U, Boeuf J, J S T, Kushner M J, Czarnetzki U and Mason N 2012 *Journal of Physics D: Applied Physics* **45** 253001

[5] Huiskamp T 2015 *Nanosecond Pulsed Power Technology for Transient Plasma Generation* Ph.D. thesis Eindhoven University of Technology Available online: https://pure.tue.nl/ws/files/3809268/798746.pdf

[6] Nair S A 2004 *Corona plasma for tar removal* Ph.D. thesis Eindhoven University of Technology

[7] Braun D, Kuchler U and Pietsch G 1988 *Pure and Applied Chemistry* **60** 741–746

[8] Kitayama J and Kuzumoto M 1999 *Journal of Physics D: Applied Physics* **32** 3032

[9] van Heesch E J M, Winands G J J and Pemen A J M 2008 *Journal of Physics D: Applied Physics* **41** 234015

[10] Matsumoto T, Wang D, Namihira T and Akiyama H 2010 *Plasma Science, IEEE Transactions on* **38** 2639–2643

[11] Wang D, Namihira T and Akiyama H 2011 *Journal of Advanced Oxidation Technologies* **14** 131–137

[12] Matsumoto T, Wang D, Namihira T and Akiyama H 2011 *Japanese Journal of Applied Physics* **50**

[13] Fujiwara M 2006 *Japanese journal of applied physics* **45** 948

[14] Kakuta T, Yagi I and Takaki K 2015 *Japanese Journal of Applied Physics* **54** 01AG02

[15] Ono R, Nakagawa Y and Oda T 2011 *Journal of Physics D: Applied Physics* **44** 485201

[16] Namihira T, Tsukamoto S, Wang D, Katsuki S, Hackam R, Akiyama H, Uchida Y and Koike M 2000 *Plasma Science, IEEE Transactions on* **28** 434–442

[17] Huiskamp T, Beckers F J C M, van Heesch E J M and Pemen A J M 2013 *Plasma Science, IEEE Transactions on* **41** 3666–3674 ISSN 0093-3813

[18] Huiskamp T, Voeten S J, van Heesch E J M and Pemen A J M 2014 *Plasma Science, IEEE Transactions on* **42** 127–137 ISSN 0093-3813

[19] Huiskamp T, Beckers F J C M, van Heesch E J M and Pemen A J M 2014 *Plasma Science, IEEE Transactions on* **42** 859–867 ISSN 0093-3813

[20] Huiskamp T, van Heesch E J M and Pemen A J M 2015 *Plasma Science, IEEE Transactions on* **43** 444–451

[21] Malik M A and Schoenbach K H 2014 *Plasma Chemistry and Plasma Processing* **34** 93–109

[22] Samaranayake W J M, Miyahara Y, Namihira T, Katsuki S, Hackam R and Akiyama H 2001 *Dielectrics and Electrical Insulation, IEEE Transactions on* **8** 826–831

[23] Ma H and Qiu Y 2003 *Ozone Science & Engineering* **25** 127–135

[24] Simek M and Clupek M 2002 *Journal of Physics D: Applied Physics* **35** 1171

[25] Van Veldhuizen E M, Rutgers W R and Bityurin V A 1996 *Plasma Chemistry and Plasma Processing* **16** 227–247

[26] Malik M A, Kolb J F, Sun Y and Schoenbach K H 2011 *Journal of hazardous materials* **197** 220–228

[27] Clements J S, Mizuno A, Finney W C and Davis R H 1989 *Industry Applications, IEEE Transactions on* **25** 62–69

[28] Beckers F J C M, Hoeben W F L M, Pemen A J M and Van Heesch E J M 2013 *Journal of Physics D: Applied Physics* **46** 295201

[29] Mok Y S and Ham S W 1998 *Chemical engineering science* **53** 1667–1678

[30] Mizuno A, Shimizu K, Chakrabarti A, Dascalescu L and Furuta S 1995 *Industry Applications, IEEE Transactions on* **31** 957–962

[31] Wu Y, Li J, Wang N and Li G 2003 *Journal of Electrostatics* **57** 233–241
[32] Fei X, Zhongyang L, Wei C, Peng W, Bo W, Xiang G, Mengxiang F and Kefa C 2009 *Journal of Environmental Sciences* **21** 328–332
[33] Yan K, Li R, Zhu T, Zhang H, Hu X, Jiang X, Liang H, Qiu R and Wang Y 2006 *Chemical Engineering Journal* **116** 139–147
[34] Hoeben W F L M, Beckers F J C M, Pemen A J M, van Heesch E J M and Kling W L 2012 *Journal of Physics D: Applied Physics* **45** 055202
[35] Vandenbroucke A M, Morent R, De Geyter N and Leys C 2011 *Journal of hazardous materials* **195** 30–54
[36] Yamamoto T, Ramanathan K, Lawless P A, Ensor D S, Newsome J R, Plaks N and Ramsey G H 1992 *Industry Applications, IEEE Transactions on* **28** 528–534
[37] Nunez C M, Ramsey G H, Ponder W H, Abbott J H, Hamel L E and Kariher P H 1993 *Air & Waste* **43** 242–247
[38] Tippayawong N and Inthasan P 2010 *International Journal of Chemical Reactor Engineering* **8**
[39] Winands G J J, Yan K, Pemen A J M, Nair S A, Liu Z and Van Heesch E J M 2006 *Plasma Science, IEEE Transactions on* **34** 2426–2433
[40] Okubo M, Kametaka H, Yoshida K and Yamamoto T 2007 *Japanese Journal of Applied Physics* **46** 5288
[41] Park C W, Byeon J H, Yoon K Y, Park J H and Hwang J 2011 *Separation and Purification Technology* **77** 87–93
[42] Liang Y, Wu Y, Sun K, Chen Q, Shen F, Zhang J, Yao M, Zhu T and Fang J 2012 *Environmental science & technology* **46** 3360–3368
[43] Kelly-Wintenberg K, Sherman D M, Tsai P Y, Gadri R B, Karakaya F, Chen Z, Reece Roth J and Montie T C 2000 *Plasma Science, IEEE Transactions on* **28** 64–71
[44] Vaze N D, Gallagher M J, Park S, Fridman G, Vasilets V N, Gutsol A F, Anandan S, Friedman G and Fridman A A 2010 *Plasma Science, IEEE Transactions on* **38** 3234–3240
[45] Park G Y, Park S J, Choi M Y, Koo I G, Byun J H, Hong J W, Sim J Y, Collins G J and Lee J K 2012 *Plasma Sources Science and Technology* **21** 043001
[46] Wojtowicz J A 1996 *Kirk-Othmer encyclopedia of chemical technology*
[47] Winands G G J 2007 *Efficient Streamer Plasma Generation* Ph.D. thesis Eindhoven University of Technology
[48] Masuda S, Sato M and Seki T 1986 *Industry Applications, IEEE Transactions on* 886–891
[49] Wang D, Matsumoto T, Namihira T and Akiyama H 2010 *Journal of Advanced Oxidation Technologies* **13** 71–78
[50] Huiskamp T, Beckers F J C M, Hoeben W F L M, van Heesch E J M and Pemen A J M 2016 *Plasma Sources Science and Technology* **25** 054006
[51] Sathiamoorthy G, Kalyana S, Finney W C, Clark R J and Locke B R 1999 *Industrial & engineering chemistry research* **38** 1844–1855
[52] Yamamoto T, Yang C L, Beltran M R and Kravets Z 2000 *Industry Applications, IEEE Transactions on* **36** 923–927
[53] Whitehead J C 2010 *Pure and Applied Chemistry* **82** 1329–1336
[54] Chen H L, Lee H M, Chen S H, Chang M B, Yu S J and Li S N 2009 *Environmental science & technology* **43** 2216–2227
[55] Chirumamilla V R, Hoeben W F L M, Beckers F J C M, Huiskamp T and Pemen A J M 2016 *Plasma chemistry and plasma processing* **36** 487–510
[56] Huiskamp T, Beckers F J C M, van Heesch E J M and Pemen A J M 2016 *IEEE Sensors Journal* **16** 3792–3801
[57] Huiskamp T, Sengers W and Pemen A J M 2016 *Review of Scientific Instruments* **87** 123509
[58] Smulders E H W M, Van Heesch B E J M and van Paasen S S V B 1998 *Plasma Science, IEEE Transactions on* **26** 1476–1484
[59] Griffiths P R and De Haseth J A 2007 *Fourier transform infrared spectrometry* vol 171 (John

Wiley & Sons)

[60] Shimomura N, Wakimoto M, Togo H, Namihira T and Akiyama H 2003 Production of ozone using nanosecond short pulsed power *Pulsed Power Conference, 2003. Digest of Technical Papers. PPC-2003. 14th IEEE International* vol 2 (IEEE) pp 1290–1293

[61] Eliasson B and Kogelschatz U 1991 *Plasma Science, IEEE Transactions on* **19** 309–323

[62] Huiskamp T, Sengers W, Beckers F J C M, Nijdam S, Ebert U, van Heesch E J M and Pemen A J M 2017 *Plasma Sources Science and Technology* **26** 075009 (1–19)

[63] Eichwald O, Ducasse O, Dubois D, Abahazem A, Merbahi N, Benhenni M and Yousfi M 2008 *Journal of Physics D: Applied Physics* **41** 234002

[64] Ono R and Oda T 2004 *Journal of Physics D: Applied Physics* **37** 730

[65] Komuro A, Takahashi K and Ando A 2015 *Journal of Physics D: Applied Physics* **48** 215203

[66] Orlandini I and Riedel U 2000 *Journal of Physics D: Applied Physics* **33** 2467